Title

Phosphorylation of Ser1928 mediates the enhanced activity of the L-type Ca2+ channel Cav1.2 by the β2-adrenergic receptor in neurons

Journal

Science Signaling, 10(463)

ISSN

1945-0877

Authors

Qian, Hai
Patriarchi, Tommaso
Price, Jennifer L
et al.

Publication Date

2017-01-24

DOI

10.1126/scisignal.aaf9659

Peer reviewed

HHS Public Access

Author manuscript

Sci Signal. Author manuscript; available in PMC 2017 February 15.

Published in final edited form as:

Sci Signal. ; 10(463): . doi:10.1126/scisignal.aaf9659.

Phosphorylation of Ser^{1928} mediates the enhanced activity of the L-type Ca^{2+} channel $Ca_v1.2$ by the β_2-adrenergic receptor in neurons

Hai Qian[1,*], **Tommaso Patriarchi**[2], **Jennifer L. Price**[2], **Lucas Matt**[2,†], **Boram Lee**[2], **Madeline Nieves-Cintrón**[2], **Olivia R. Buonarati**[2], **Dhrubajyoti Chowdhury**[2], **Evanthia Nanou**[3], **Matthew A. Nystoriak**[2,‡], **William A. Catterall**[3], **Montatip Poomvanicha**[4], **Franz Hofmann**[4], **Manuel F. Navedo**[2,§], and **Johannes W. Hell**[1,2,§]

[1]Department of Pharmacology, University of Iowa, Iowa City, IA 52242–1109, USA

[2]Department of Pharmacology, University of California, Davis, CA 95616–8636, USA

[3]Department of Pharmacology, University of Washington, Seattle, WA 98195–7280, USA

[4]Department of Pharmacology and Toxicology, Technical University of Munich, D-80802 Munich, Germany

Abstract

The L-type Ca^{2+} channel $Ca_v1.2$ controls multiple functions throughout the body including heart rate and neuronal excitability. It is a key mediator of fight-or-flight stress responses triggered by a signaling pathway involving β-adrenergic receptors (βARs), cyclic adenosine monophosphate (cAMP), and protein kinase A (PKA). PKA readily phosphorylates Ser^{1928} in $Ca_v1.2$ in vitro and in vivo, including in rodents and humans. However, S1928A knock-in (KI) mice have normal PKA-mediated L-type channel regulation in the heart, indicating that Ser^{1928} is not required for regulation of cardiac $Ca_v1.2$ by PKA in this tissue. We report that augmentation of L-type currents by PKA in neurons was absent in S1928A KI mice. Furthermore, S1928A KI mice failed to induce long-term potentiation in response to prolonged theta-tetanus (PTT-LTP), a form of synaptic plasticity that requires $Ca_v1.2$ and enhancement of its activity by the β_2-adrenergic receptor

[§]Corresponding author. mfnavedo@ucdavis.edu (M.F.N.); jwhell@ucdavis.edu (J.W.H.).
[*]Present address: Genocoon LLC, Chadds Ford, PA 19317, USA.
[†]Present address: Department of Pharmacology, Toxicology and Clinical Pharmacy, Institute of Pharmacy, University of Tübingen, Auf der Morgenstelle 8, D-72076 Tübingen, Germany.
[‡]Present address: Diabetes and Obesity Center, Department of Medicine, University of Louisville, 580 South Preston Street, Delia Baxter, Louisville, KY 40202, USA.

Author contributions: J.W.H. developed the research strategy; M.F.N. and J.W.H. oversaw the project and interpretation of the experimental data; H.Q., T.P., J.L.P., L.M., M.N.-C., B.L., O.R.B., D.C., E.N., M.P., and M.F.N. performed the experiments; F.H. provided the S1928A KI mice; W.A.C. provided the STAA mice; H.Q., T.P., J.L.P., M.N.-C., B.L., L.M., E.N., M.P., M.A.N., and M.F.N. analyzed the data; H.Q., T.P., J.L.P., L.M., M.P., and M.F.N. prepared figures; and H.Q., T.P., W.A.C., F.H., M.F.N., and J.W.H. wrote the manuscript.

Competing interests: The authors declare that they have no competing interests.

Data and materials availability: The mutant mice require a material transfer agreement from the University of Munich (S1928A KI mice) or the University of Washington (STAA mice).

SUPPLEMENTARY MATERIALS
www.sciencesignaling.org/cgi/content/full/10/463/eaaf9659/DC1

(β_2AR)–cAMP–PKA cascade. Thus, there is an unexpected dichotomy in the control of $Ca_v1.2$ by PKA in cardiomyocytes and hippocampal neurons.

INTRODUCTION

$Ca_v1.2$ is the most abundant L-type Ca^{2+} channel in mammalian brain, heart, and vascular smooth muscle (1–4) regulating neuronal excitability, cardiac contractility, and vascular tone. Mutations in $Ca_v1.2$ affect many organs, as illustrated by the cardiac arrhythmias, autistic-like behavior, and developmental abnormalities in Timothy syndrome patients, who have gain-of-function mutations in $Ca_v1.2$ (5).

In the brain, L-type Ca^{2+} currents control neuronal excitability (6, 7), gene expression (8–11), and long-term potentiation (LTP) of synaptic strength. LTP refers to the persistent increase in synaptic strength that a synapse undergoes when it experiences a period of high-frequency activation (12–14). LTP is a key cellular correlate of learning and memory. In particular, L-type Ca^{2+} currents conducted by the voltage-gated calcium channel $Ca_v1.2$ are important for LTP induced by the widely used 1-s-long, 200-Hz tetanus (15, 16) or by a 90- to 180-s-long, 5- to 10-Hz tetanus mimicking the endogenous ~7-Hz theta rhythm, which we call prolonged theta-tetanus LTP (PTT-LTP) (17). Ca^{2+} influx through $Ca_v1.2$ is also important for long-term depression (LTD) induced by metabotropic glutamate receptor (mGluR) signaling (18). LTD is a persistent decrease in synaptic strength induced by a prolonged stimulation of a synapse with a frequency in the range of 1 Hz (18).

Norepinephrine is important for wakefulness, behavioral acuity, and various forms of learning, especially in novel or emotionally charged situations (19–23). Norepinephrine activates adenylyl cyclase (AC)–cyclic adenosine monophosphate (cAMP)–protein kinase A (PKA) signaling by the β_1- and β_2-adrenergic receptors (β_1AR and β_2AR) (24). This signaling cascade stimulates Ca^{2+} influx through $Ca_v1.2$ into neurons (25–28) and cardiomyocytes (29, 30).

Vertebrate $Ca_v1.2$ is composed of the pore-forming $\alpha_1 1.2$ subunit, a so-called α_2-δ subunit, and a β subunit (2, 31). $\alpha_1 1.2$ consists of a cytosolic N terminus, the four homologous domains I to IV, each with six transmembrane segments, and the long C terminus of ~660 residues. Injection of active PKA into cells exogenously expressing $\alpha_1 1.2$ without the other subunits increases channel activity (32), suggesting that PKA acts directly on $\alpha_1 1.2$. In purified preparations of $Ca_v1.2$ channels, Ser^{1928} in the distal C-terminal domain is the most readily detectable site of PKA phosphorylation (33–36). βAR stimulation with isoproterenol (ISO) results in a pronounced increase in Ser^{1928} phosphorylation in isolated cardiomyocytes (37) and in the brain in vivo (38) [see also (39, 40)]. However, functional studies in transfected nonmuscle cells indicate that phosphorylation of Ser^{1700} in the proximal C-terminal domain increases $Ca_v1.2$ channel activity, whereas phosphorylation of Ser^{1928} in the distal C-terminal domain does not (41). Moreover, studies of $Ca_v1.2$ regulation in virally transfected cardiac myocytes and in ventricular myocytes dissociated from knock-in (KI) mice in which Ser^{1928} has been mutated to alanine (S1928A KI mice) show that βAR stimulation of L-type currents is normal when Ser^{1928} is mutated to alanine (42, 43).

In the brain and heart, the β_2AR forms a signaling complex with $Ca_v1.2$ that also contains AC, the heterotrimeric guanine nucleotide–binding protein (G protein) G_s, an A-kinase anchoring protein (AKAP), and PKA (10, 25, 28, 29, 35, 38, 41, 44–47). This complex allows highly localized and thereby effective and specific signaling from the β_2AR to $Ca_v1.2$ in neurons (25) and cardiomyocytes (29, 48) [for a review, see (24)]. The β_2AR binds to $\alpha_1$1.2 residues 1923 to 1942, and this interaction is strictly required for receptor-mediated regulation of $Ca_v1.2$ (17). Furthermore, stimulating the β_2AR leads to its temporary displacement from $Ca_v1.2$, creating a refractory period of ~5 min, during which neither phosphorylation nor channel activity of $Ca_v1.2$ can be augmented again by restimulation of the β_2AR (17). When we tested whether such a refractory period for sequential β_2AR stimulation would be observed in S1928A KI mice, we discovered that βAR stimulation did not augment neuronal L-type currents in these mice. In further contrast to cardiomyocytes, we found that, in neurons, L-type currents were exclusively augmented by β_2AR but not by β_1AR stimulation. Finally, we demonstrated that this Ser^{1928}-dependent regulation of L-type Ca^{2+} currents was a key requirement for the induction of stable PTT-LTP by theta rhythm stimulation in the presence of a βAR agonist. Collectively, our results demonstrated a bifurcation of PKA signaling to $Ca_v1.2$ channels and define a new phosphorylation site that is required for LTP. Furthermore, they revealed that phosphorylation of a single site, Ser^{1928}, not only uncouples $Ca_v1.2$ regulation from β_2AR signaling upon repeated stimulation but also mediates the channel-stimulating response to β_2AR signaling in hippocampal neurons.

RESULTS

Increase in L-type Ca^{2+} currents upon βAR stimulation depends on Ser^{1928} in neurons

In neurons, phosphorylation of Ser^{1928} upon βAR stimulation displaces the β_2AR from $Ca_v1.2$ for ~5 min. A second application of the βAR agonist ISO only increases L-type currents in neurons if added more than 5 min after the first application has ended (17). In neuronal cultures from the hippocampal CA1, CA2, and CA3 regions, augmentation of L-type currents by ISO is much more apparent in cell-attached recordings, which typically yield increases of >200% (17, 25, 27), than in whole-cell recordings, which only show increases of 10 to 20% (27, 28). The weak ISO effect in whole-cell recordings from neurons is much smaller than in whole-cell recordings from cardiomyocytes (43). To functionally test whether Ser^{1928} phosphorylation mediates this refractory period of L-type current augmentation, we recorded single-channel L-type currents from hippocampal neurons cultured from wild-type and S1928A KI mice by cell-attached patch-clamping (Fig. 1A), using conditions as previously described (17, 25).

We determined open probability (Po) for all L-type channels within each patch (NPo) during depolarizing pulses from −80 to 0 mV with ω-conotoxins GVIA and MVIIC in the patch pipette to blocked non–L-type Ca^{2+} currents (Fig. 1B) (17). In neurons from wild-type mice, the addition of ISO to the patch pipette significantly increased NPo (Fig. 1, A and B). This increase was also evident in neurons prepared from only the hippocampal CA1 region, avoiding the CA2 and CA3 regions, from wild-type mice (fig. S1). In neurons from S1928A KI mice, however, the NPo value under control conditions was not significantly changed by ISO application (Fig. 1). Given that cardiac L-type currents measured in S1928A KI mice

were significantly increased by βAR signaling (43), this result in neurons was unexpected. Thus, we confirmed under our experimental conditions that there was no difference in basal L-type currents between cardiomyocytes from wild-type and S1928A KI mice (fig. S2, A and B), and potentiation by ISO was equally strong for both genotypes (fig. S2, C to G).

Signaling by the β_2AR but not the β_1AR augments L-type currents in neurons

In cardiomyocytes, L-type currents are mainly enhanced by β_1ARs with a much smaller contribution by β_2ARs (29, 37, 48–52). To test the role of these two receptors in regulating neuronal $Ca_v1.2$, we applied ISO (a nonselective βAR agonist) during cell-attached recordings in wild-type rat hippocampal neurons in the absence or presence of CGP20712 (a β_1AR-specific antagonist) or ICI118551 (a β_2AR-specific antagonist) (53). Blocking β_2AR with ICI118551 completely blocked the ISO-induced increase in NPo (Fig. 2, A and B, and fig. S1), whereas blocking β_1AR CGP20712 had no effect (Fig. 2, A and B).

Signaling by the β_2AR but not the β_1AR promotes phosphorylation of $\alpha_1$1.2 subunits in hippocampal neurons

The importance of β_2AR for the regulation of $Ca_v1.2$ in neurons was further confirmed by biochemical analysis (Fig. 3, A and B, top). Treatment of acutely isolated murine forebrain slices with ISO for 5 min significantly increased phosphorylation of Ser^{1928} and also Ser^{1700}. These effects were completely blocked by ICI118551 but unaffected by CGP20712. The increase in ISO-induced Ser^{1928} phosphorylation and its significant inhibition by ICI118551 were also observed when only the hippocampal CA1 region was used for such analysis (fig. S3). These results indicate that, in neurons in the forebrain and hippocampus, and specifically in those from the CA1 region, βAR signaling of $Ca_v1.2$ occurs through the β_2AR but not through the β_1AR.

To confirm the specificity of the antagonists for β_2AR and β_1AR and that both receptors are present and active in the neurons, we also analyzed the effect of these drugs on ISO-induced phosphorylation of AMPA-type glutamate receptor (AMPAR) subunits and *N*-methyl-D-aspartate (NMDA)–type glutamate receptor (NMDAR) subunits. The AMPAR subunit GluA1 is phosphorylated on Ser^{845} through a β_2AR-dependent pathway (17, 53–55), and the NMDAR subunit GluN2B is phosphorylated on Ser^{1166} through a β_1AR-dependent pathway (Fig. 3).

The AMPAR forms a signaling complex analogous to $Ca_v1.2$ containing β_2AR, G_s, AC, AKAP, and PKA to enable highly localized signaling by cAMP (54, 55). In this complex, the β_2AR is linked to the AMPAR GluA1 subunit through the scaffold protein PSD-95 and AMPAR subunits known as transmembrane AMPAR regulatory proteins (TARPs) (54). Phosphorylation of GluA1 on Ser^{845} in this complex augments postsynaptic strength by increasing channel activity of the AMPAR (56) and its postsynaptic accumulation (24, 54, 57–67). ICI118551 completely blocked the ISO-induced increase in the phosphorylation of the GluA1 subunit of the AMPAR on Ser^{845}, but there was minimal effect of CGP20712 (Fig. 3, A and B, bottom).

Phosphorylation of the NMDAR subunit GluN2B on Ser^{1166} by PKA selectively increases Ca^{2+} permeability of the NMDAR (68, 69). The ISO-induced increase in Ser^{1166}

phosphorylation was not blocked by ICI118551, but it was completely eliminated by CGP20712 (Fig. 3, A and B, bottom). Thus, in contrast to $Ca_v1.2$ and GluA1, these data showed that NMDAR phosphorylation is mediated by the β_1AR and not by the β_2AR. These results could reflect differential β-adrenergic signaling in individual neurons, or the differential effects of β_1AR versus β_2AR signaling could occur in different subcellular regions or different neuronal subtypes, because our forebrain slices consist of a mixture of cells. Furthermore, these results demonstrated that CGP20172 effectively blocked the β_1AR. Therefore, its lack of effect on $Ca_v1.2$ and GluA1 phosphorylation reflects the requirement for β_2AR activation and not the lack of efficacy of the drug treatment (53).

Induction of PTT-LTP requires channel activity of $Ca_v1.2$

Extended stimulation of the Schaffer collateral pathway, which originates in the hippocampal CA3 region and projects to the CA1 region, at 5–10 Hz induces PTT-LTP but only if β-adrenergic stimulation occurs at the same time (22, 53, 70, 71). This stimulation pattern is especially relevant because it mimics the naturally occurring theta rhythm (~7 Hz) (72). During the first 5 min of stimulation, which include 3 min for delivery of the 5-Hz tetanus, synaptic transmission shows an initial depression before it recovers from what might be desensitization of the postsynaptic response, and the potentiation develops during the subsequent 5 min (22, 53, 70).

The complete inhibition of PTT-LTP by ICI118551 and not by CGP20712 (53) indicates that ISO acts through β_2AR but not through β_1AR during PTT-LTP. Because β_2AR stimulation prominently augments Ca^{2+} influx through $Ca_v1.2$ at postsynaptic sites (73), we tested whether $Ca_v1.2$ and its enhancement by the β_2AR are required for PTT-LTP. We recently found that PTT-LTP is absent in conditional forebrain $Ca_v1.2$ knockout (KO) mice (17). $Ca_v1.2$ KO mice could have altered synaptic signaling due to changes in gene expression rather than electrophysiological changes that acutely contribute to PTT-LTP. We used acute pharmacological inhibition of L-type channels and NMDARs, both of which are main conduits for Ca^{2+} influx during many forms of synaptic plasticity (12–14), to evaluate their respective contributions. Whereas the competitive glutamate site antagonist aminophosphonovaleric acid (APV) significantly reduced PTT-LTP, the pore blocker MK801 had a more modest, nonsignificant effect (Fig. 4, A and B). Standard LTP induced by a single 100-Hz tetanus, which strictly requires NMDARs, was fully abrogated by either drug, indicating that both drugs effectively blocked the NMDAR in these experiments (Fig. 4, C and D). The L-type Ca^{2+} channel blocker isradipine significantly reduced PTT-LTP to a degree that appeared to be larger than that by APV or MK801. Although these differences in PTT-LTP did not reach statistical significance (Fig. 4, A and B; $P = 0.0806$ for ISO + isradipine versus ISO + APV and $P = 0.0591$ for ISO + isradipine versus ISO + MK801, Mann-Whitney test), they collectively suggested that Ca^{2+} influx through L-type channels plays a more prominent role in PTT-LTP than Ca^{2+} influx through NMDARs under our experimental conditions.

Isradipine, which is also known as PN200-110 when tritiated, is selective for L-type Ca^{2+} channels but binds multiple members of this class of channels, not only $Ca_v1.2$ (1). Hippocampal neurons also contain the L-type Ca^{2+} channel $Ca_v1.3$, albeit at a much lower

amount than $Ca_v1.2$ (1, 3). Therefore, the effect of isradipine may have resulted from blocking $Ca_v1.3$ rather than $Ca_v1.2$ or by blocking both channels. Mutating Thr^{1066} to Tyr in the $\alpha_1 1.2$ subunit makes $Ca_v1.2$ insensitive to dihydropyridines such as isradipine (3). We used T1066Y KI mice (3) to scrutinize whether isradipine inhibited PTT-LTP by blocking $Ca_v1.2$ rather than $Ca_v1.3$. Isradipine blocked PTT-LTP in litter-matched wild-type mice but not in homozygous dihydropyridine-insensitive T1066Y KI mice (Fig. 5). These results indicated that induction of PTT-LTP depends on $Ca_v1.2$ channel activity.

Phosphorylation of $Ca_v1.2$ on Ser^{1928} is required for PTT-LTP

Given that the β_2AR and $Ca_v1.2$ are required for PTT-LTP and that Ser^{1928} is needed for augmenting $Ca_v1.2$ activity, we hypothesized that PTT-LTP depends on phosphorylation of Ser^{1928} by PKA downstream of the β_2AR. PTT-LTP was absent 30 to 60 min after a theta burst stimulus in slices from S1928A KI mice, whereas it was readily induced in litter-matched control wild-type mouse slices (Fig. 6). In hippocampal slices from mice of each genotype, after the typical initial reversal of the depression of synaptic transmission seen during the theta tetanus, synaptic strength returned to the baseline level seen before PTT-LTP induction and then increased above the baseline up to 15 min after stimulation (Fig. 6A). However, after 15 min, synaptic strength declined to below control values for S1928A mice, whereas it remained increased for at least 60 min in controls (Fig. 6B).

Input-output curves for increased stimulus strength versus field excitatory postsynaptic potential (fEPSP) response strength, an indication of postsynaptic glutamate receptor activity, and paired-pulse facilitation, an indication of presynaptic glutamate release function, did not show any differences between slices from S1928A KI mice and those from litter-matched wild-type control mice over a wide range of values (fig. S4). Accordingly, basal synaptic transmission including presynaptic glutamate release and postsynaptic glutamate receptor activity appear unaltered in S1928A KI mice.

Both the PKA-targeted site Ser^{1700} and the nearby residue Thr^{1704} are implicated in the regulation of $Ca_v1.2$ (41, 74–76). We analyzed PTT-LTP in S1700A/T1704A double KI mice (“STAA mice”). There was no difference in PTT-LTP between slices from STAA mice and litter-matched wild-type mice (fig. S5). In addition, input-output curves for fEPSP responses and paired-pulse facilitation were comparable for these two genotypes (fig. S6). We concluded that induction of PTT-LTP requires increased $Ca_v1.2$ activity mediated by β_2AR-PKA signaling through Ser^{1928} phosphorylation but not through Ser^{1700} or Thr^{1704} phosphorylation.

DISCUSSION

Regulation of the L-type Ca^{2+} channel $Ca_v1.2$ by βAR-cAMP-PKA signaling plays a prominent role in mediating the fight-or-flight response of our heartbeat, as triggered by norepinephrine (29, 30, 77, 78). Signaling by norepinephrine through this pathway also augments arousal, behavioral acuity, and emotionally motivated learning (19–23). A prominent target of norepinephrine action in the brain is $Ca_v1.2$, which forms a complex with the β_2AR, G_s, AC, AKAPs, and PKA (24–26, 28, 29). In turn, $Ca_v1.2$ controls neuronal excitability through closely associated Ca^{2+}-activated K^+ channels (6, 7). Ca^{2+} influx

through $Ca_v1.2$ is more effective in regulating gene expression through the cAMP response element–binding protein and nuclear factor of activated T cells than Ca^{2+} influx through other Ca^{2+} channels (8–11), and $Ca_v1.2$-induced Ca^{2+} influx is important for various forms of synaptic plasticity (15, 16, 18). Yet, the molecular mechanism by which PKA increases ion flux through $Ca_v1.2$ in the brain and heart remains incompletely defined. We identified Ser^{1928} of $Ca_v1.2$ as an essential PKA-regulated site important for PTT-LTP. Furthermore, we found differential regulation of $Ca_v1.2$ by the PKA pathway in the brain and heart. Parallel work on the regulation of $Ca_v1.2$ by PKA in vascular smooth muscle cells (VSMCs) also shows that this regulation is completely abrogated in S1928A KI mice (79).

The findings in neurons and VSMCs are in striking contrast to cardiomyocytes, in which Ser^{1928} in the distal C-terminal domain does not seem to be involved; rather, phosphorylation of Ser^{1700} in the proximal C-terminal domain has been implicated in the increase in channel activity of cardiac $Ca_v1.2$ by βAR signaling (41, 74–76). In neurons, we found that the β_2AR-specific blocker ICI118551 completely blocked the ISO-induced increase in NPo of $Ca_v1.2$, whereas blocking β_1AR with CGP20712 had no effect. In contrast, cardiac $Ca_v1.2$ channels are primarily regulated by β_1AR signaling (29, 37, 48–52). Although β_2ARs are present in rodent and human heart, they do not participate in the increase in $Ca_v1.2$ channel activity that augments contractility in the flight-or-flight response. Accordingly, the βAR-mediated regulation of $Ca_v1.2$ in the heart and brain depends on different βAR subtypes and phosphorylation of different sites on $Ca_v1.2$.

β_2AR regulation of $Ca_v1.2$ channels in the heart is thought to occur mostly in caveolae and to be important for initiation of cardiac hypertrophy in response to hypertrophic signals (80). The β_1AR and β_2AR engage different downstream effectors in the G protein and arrestin pathways through biased signaling (81, 82), and these different signaling pathways may lead to biased changes in phosphorylation status of $Ca_v1.2$ channels in the heart and brain. More work is required to determine how these two signaling pathways can engage regulation of $Ca_v1.2$channels through phosphorylation of Ser^{1928} versus Ser^{1700} and Thr^{1704}. Some possible mechanisms for the different regulation of $Ca_v1.2$ in the brain and heart include differential subunit composition of the channel, differential proteolytic processing of the channel, and differential association of the channel with AKAPs in the brain and heart.

Four different genes encode $\alpha_2\delta$ subunits ($\alpha_2\delta_1$ to $\alpha_2\delta_4$) and β subunits (β_1 to β_4), which further undergo differential splicing (83, 84). In cardiomyocytes, β_2 is functionally the most prominent β subunit in defining the biophysical properties of $Ca_v1.2$ (85). β_{2A} is phosphorylated by PKA on Ser^{459}, Ser^{478}, and Ser^{479}, which are not present in the β_1, β_3, or β_4 subunit (86). Although there is evidence that Ser^{478} and Ser^{479} are not required for increased $Ca_v1.2$ activity in virally infected ventricular myocytes (42), this system does not fully reconstitute β-adrenergic regulation of L-type currents, leaving open the possibility that Ser^{478} and Ser^{479} contribute to the increase of L-type currents in the heart. In the brain, all four β subunits are broadly expressed (87–89). Thus, it is conceivable that PKA-regulated phosphorylation of β_2 compensates for the loss of Ser^{1928} phosphorylation in S1928A KI mice in cardiomyocytes but not neurons. It is also possible that differential splicing of $\alpha_1$1.2 plays a role, although all known splice variants are predicted to contain Ser^{1928} (90, 91).

In cardiomyocytes, $\alpha_1$1.2 is proteolytically processed, and this processing and subsequent noncovalent association of the cleaved C-terminus with the channel core are required for PKA-dependent regulation (41, 46). Reconstitution of regulation of a cardiac form of Ca_v1.2 by PKA in cultured nonmuscle cells requires formation of an autoinhibitory signaling complex composed of the core of the Ca_v1.2 channels with the noncovalently bound cleaved portion (41), which makes analysis of PKA-dependent regulation in this system challenging. Ca_v1.2 channels are not as extensively proteolytically processed in hippocampal neurons as in the heart, unless massive Ca^{2+} influx is induced by prolonged activation of NMDA receptors (33, 92). Therefore, differences in proteolytic processing and assembly of the Ca_v1.2 signaling complex in the heart and brain may contribute to the differences in mechanisms of PKA regulation.

Regulation of Ca_v1.2 channels in the heart and brain requires AKAPs to anchor PKA (10, 28, 35, 38, 41, 44–47). Differential regulation of Ca_v1.2 channels can be induced in reconstituted nonmuscle cells by coexpression of different AKAPs (93). Association of Ca_v1.2 channels with different sets of AKAPs in the brain and heart might contribute to differential channel regulation by PKA phosphorylation of distinct sites.

Another important finding was that PTT-LTP depends on Ca_v1.2 and its phosphorylation of Ser^{1928} but not Ser^{1700}. PTT-LTP is thought to underlie contextual learning under difficult or stressful situations (22). PTT-LTP requires simultaneous stimulation by prolonged theta tetanus and β_2AR signaling (22, 53, 70). The β_2AR forms two distinct signaling complexes with postsynaptic ion channels, namely, AMPARs and Ca_v1.2, and both are now emerging as critical targets for β_2AR-PKA signaling during PTT-LTP (17, 53, 63).

The β_2AR binds to the scaffold protein PSD-95, which, in turn, binds to the AMPAR (54, 55). In addition, AKAP150, which is associated with GluA1 through SAP97 (94), recruits AC (65, 95), PKA, and the phosphatase PP2B to the AMPAR complex (24, 62, 63, 65, 96–98). The close proximity of all components of this cAMP cascade in this AMPAR complex and the analogous β_2AR-G_s-AC-PKA-Ca_v1.2 complex results in highly localized, selective, and potent augmentation of channel activity of AMPARs and Ca_v1.2 by cAMP (17, 25, 29, 47, 48, 54). Phosphorylation of Ca_v1.2 on Ser^{1928} and of the AMPAR GluA1 subunit on Ser^{845}, which is also required for PTT-LTP (53), might synergistically augment Ca^{2+} influx into postsynaptic sites through Ca_v1.2 in PTT-LTP (Fig. 7). During PTT-LTP, stimulation of the β_2AR results in phosphorylation of Ser^{845}, which increases AMPAR Po (56, 97) and promotes postsynaptic accumulation of GluA1-containing AMPARs (54, 57, 58, 60). Consequently, Na^+ influx increases, resulting in depolarization of postsynaptic sites during PTT-LTP. In addition, we found that phosphorylation of Ser^{1928} increases the Po of Ca_v1.2. In other cell types, Ca_v1.2 phosphorylation at Ser^{1928} also shifts the activation threshold for Ca_v1.2 toward more negative membrane potentials (fig. S2) (27, 32, 37, 43, 75, 76). This leftward shift means that less depolarization is required for channel opening. In addition, it further increases Ca^{2+} influx because the driving force for this Ca^{2+} influx is larger at these more negative potentials. The combined effect of Ser^{845} and Ser^{1928} phosphorylation would thereby be stronger Ca^{2+} influx through Ca_v1.2.

The time course of PTP-LTP after the theta tetanus train in S1928A mice initially showed an increase in synaptic strength above aseline, but eventually, postsynaptic responses fell below those of wild-type controls (Fig. 6). It is possible that, in the absence of the ISO-induced increase in $Ca_v1.2$ activity through Ser^{1928} phosphorylation, PKA phosphorylation of Ser^{845} in GluA1 in the AMPAR is sufficient to initially enhance synaptic strength. However, without augmented Ca^{2+} entry through the $Ca_v1.2$ channels, the neurons ultimately respond with synaptic depression. Such coincidence detection of depolarization through AMPAR and Ca^{2+} entry mediated by $Ca_v1.2$ channels could be a mechanism to ensure precise capture of incoming signals that lead to LTP.

In contrast to the S1928A KI mice, a decrease in synaptic transmission upon PTT-LTP induction was not seen in slices from S845A KI mice, although PTT-LTP was also impaired in S845A KI slices (53). Perhaps in the absence of increased Ca^{2+} influx through $Ca_v1.2$ in the S1928A slices, mechanisms that induce NMDAR-dependent LTD prevail, which requires Ser^{845} phosphorylation for temporary insertion of Ca^{2+}-permeable AMPARs into the postsynaptic membrane (63). Another potential explanation is that, in S1928A KI mice, the constitutive absence of the increase in $Ca_v1.2$ activity upon βAR receptor signaling affects gene expression in a way that influences postsynaptic signaling during PTT-LTP. The absence of PTT-LTP in S1928A KI mice is consistent with an essential role of Ser^{1928} phosphorylation in the increase in $Ca_v1.2$ channel activity by β_2AR signaling because PTT-LTP depends on both β_2AR and $Ca_v1.2$ (17, 53). In summary, we demonstrate that Ser^{1928} phosphorylation of $Ca_v1.2$ is required for augmentation of $Ca_v1.2$ channel activity by β_2AR stimulation and that this mechanism constitutes a critical component of the molecular mechanism underlying stable PTT-LTP.

MATERIALS AND METHODS

Animals

All procedures involving animals followed the guidelines for the Care and Use of Laboratory Animals of the National Institutes of Health and had been approved by the Institutional Animal Care and Use committees at the University of California, Davis, and the University of Washington. S1928A KI mice were described in (43), and STAA mice were described in (75).

Reagents, peptides, and antibodies

ISO in the form of ISO bitartrate salt, ICI118551, CGP20712, and microcystin LR were from Sigma-Aldrich; protein A–coated beads were from Repligen; polyvinyldene fluoride (PVDF) membranes were from Millipore; horseradish peroxidase (HRP)–coupled protein A and enhanced chemiluminescence (ECL) reagents were from GE Healthcare; EGTA, EDTA, Tween 20, Triton X-100, and tris were from Thermo Fisher Scientific; and ω-conotoxins GVIA and MCVIIC were from Bachem. (*S*)-(−)-Bay K8644 was from Millipore, and isradipine was from Enzo Life Sciences. Other reagents were from the typical suppliers and of standard quality. Antibodies against $\alpha_1$1.2 (FP1), $pSer^{1700}$, $pSer^{1928}$, GluA1, and $pSer^{845}$ are exactly as detailed (17). Antibodies against GluN2B and $pSer^{1166}$ are described in (69).

Preparation of brain slices and use for biochemical analysis

Eight- to 12-week-old mice with a genetic background of 50% C57BL/6 and 50% S129/Sv (S1928A KI mice) or mostly C57BL/6 (STAA, back-crossed at least four times with C57BL/6) were decapitated, and brains placed into ice-cold artificial cerebrospinal fluid (ACSF) (127 mM NaCl, 26 mM $NaHCO_2$, 1.2 mM KH_2PO_4, 1.9 mM KCl, 2.2mM$CaCl_2$,1mM $MgSO_4$, and 10 mM D-glucose; 290 to 300 mosmol/kg; saturated with 95% O_2 and 5% CO_2; final pH 7.3). About one-third of the rostral and caudal portions of the brain were trimmed off. Forebrain slices (350 μm thick) containing the hippocampus were prepared with a vibratome (Leica VT 1000A) and equilibrated in oxygenated ACSF for 1 hour at 30°C before transfer to incubation or recording chambers.

Biochemistry

Slices were equilibrated for 30 min at 32°C and treated with the various drugs for 5 min. Slices were processed with a glass Teflon homogenizer in a 10-fold excess (v/w) of immunoprecipitation buffer [1% Triton X-100, 150 mM NaCl, 10 mM EDTA, 10 mM EGTA, and 10 mM tris-HCl (pH 7.4)] (35) containing protease inhibitors [pepstatin A (1 μg/ml), leupeptin (10 μg/ml), aprotinin (20 μg/ml), and 200 nM phenylmethylsulfonyl fluoride, the latter being added immediately before homogenization and again at the start of the immunoprecipitation] and phosphatase inhibitors (2 μM microcystin LR, 1 mM *p*-nitrophenyl phosphate, 50 mM Na-pyrophosphate, and 50 mM NaF) (38, 99). Nonsolubilized material was removed by ultracentrifugation (250,000*g* for 30 min) before immunoprecipitation (4 hours at 4°C) with antibodies against $\alpha_1$1.2 (FP1; 4 μg) plus GluA1 (1 μg) and GluN2B. The protein A beads were washed three times with immunoprecipitation buffer containing 0.05% Triton X-100 plus 0.5% glycerol. SDS–polyacrylamide gel electrophoresis and transfer onto PVDF membranes were followed by blocking [5% dry milk in tris-buffered saline (TBS)], incubation with primary antibodies (5% dry milk in TBS; 1 hour), three washes with 0.05% Tween 20 in TBS, incubation with HRP–protein A (1:10,000 in 5% dry milk in TBS; 1 hour), several washes for 2 hours, and detection of HRP with ECL or ECL plus chemiluminescence reagents. Multiple exposures of increasing length ensured that signals were in the linear range, as previously described (40, 99).

Cell-attached patch-clamp recording

Primary hippocampal neurons were cultured from Sprague-Dawley rats or wild-type and S1928A KI mice, which had a 50% 129/SV and 50% C57BL/6 genetic background, of either sex, as previously described (100–102). Cell-attached patch-clamp recordings were performed after 7 to 14 days in culture, as previously described (17, 25), on an Olympus IX70 inverted microscope at 22°C. Signals were recorded at 10 kHz and low-pass–filtered at 2 kHz with an Axopatch 200B amplifier and Digidata 1440 digitizer (all from Molecular Devices). Recording electrodes were pulled from borosilicate capillary glass (outer diameter, 0.86 mm) with a Flaming micropipette puller (model P-97, Sutter Instruments) and polished (polisher from World Precision Instruments; resistance, 3.5 to 6.5 megohms). The patch transmembrane potential was zeroed by keeping neurons in high K^+ extracellular solution containing 145 mM KCl, 10 mM NaCl, and 10 mM Hepes [pH 7.4 (NaOH)] during the recordings. The pipette solution contained 20 mM tetraethylammonium chloride (TEA-Cl),

110 mM $BaCl_2$ (as charge carrier), and 10 mM Hepes [pH 7.3 (TEA-OH)] plus 1 μM ω-conotoxin GVIA and 1 μM ω-conotoxin MCVIIC to block N- and P/Q-type Ca^{2+} channels, respectively. (*S*)-(−)-Bay K8644 (500 nM) was added to the pipette solution to promote longer open times. This procedure is routinely applied to augment detection of L-type channels by single-channel recordings. Single-channel activity was recorded during an average of 50 2-s-long pulses from a holding potential of −80 to 0 mV every 5 s for each experimental condition. The single-channel event-detection algorithm of pClamp 10 was used to determine single-channel opening amplitudes and NPo. NPo values were combined for each condition and analyzed with GraphPad Prism 5.

fEPSP recording from brain slices

Recordings were from either sex, as previously described (17, 53). Slices were perfused with a flow rate of 2 ml/min at 30°C, with ACSF equilibrated with 95% O_2 and 5% CO_2 (final pH 7.3). Schaffer collaterals were stimulated every 15 s with a bipolar tungsten electrode, and resulting fEPSPs in CA1 were recorded with a glass electrode filled with ACSF. Signals were amplified with an Axopatch 2B amplifier, digitized with Digidata 1320A, and analyzed with Clampex 9 (Molecular Devices). Stimulus strength was titrated to define maximal response and input-output curves and adjusted to result in ~50% of maximal response. PTT-LTP was induced by a 3-min, 5-Hz tetanus. The average of fEPSP initial slopes from the 5 min preceding the tetanus was set to equal 100% baseline level. The PTT-LTP strength was defined as the average of fEPSP initial slopes obtained between 15 and 45 min after the tetanus. To determine paired-pulse facilitation, fEPSP initial slopes of two consecutive stimuli with the indicated interevent intervals were recorded.

Whole-cell patch-clamp recording from cardiomyocytes

Ventricular myocytes were isolated from mice of either sex, as previously described (Alliance for Cellular Signaling Procedure Protocol PP00000125) (103), maintained at 37°C, and aerated with 98% O_2 and 2% CO_2. Calcium currents (I_{Ca}) were recorded in whole-cell mode at room temperature from calcium-tolerant myocytes within 1 to 24 hours of isolation. The extracellular solution contained 137 mM NaCl, 1.8 mM $CaCl_2$, 25 mM CsCl, 0.5 mM $MgCl_2$, 10 mM Hepes, and 10 mM glucose (pH 7.4). Patch pipettes (1 to 1.5 megohms) were filled with 120 mM CsCl, 10 mM 1,2-bis(2-aminophenoxy)ethane-*N*,*N*,*N*′,*N*′-tetraacetic acid, 1 mM EGTA, 1 mM $MgCl_2$, 1 mM Na_2GTP, 5 mM phosphocreatine, and 10 mM Hepes (pH 7.2). I_{Ca} was elicited by depolarizing steps. A prepulse from −80 to −40 mV was used to inactivate fast Na^+ currents and then stepped to voltages between −40 and +60 mV (10-mV increments). I_{Ca} was recorded by an Axopatch 200B amplifier (Axon Instruments) and stored on a computer through an analog-digital converter (DIGIDATA 1332A; Axon Instruments). Protocols were controlled by pClamp 9 software (Axon Instruments). I_{Ca} was measured as the difference between the peak inward current and the current after the test pulse ended. After establishing a stable baseline, the effect of 1 μM ISO on I_{Ca} was examined.

Statistical analysis

Data are expressed as means ± SEM. Data were analyzed using GraphPad Prism software. Data were assessed for normality of distribution using the Shapiro-Wilk test. Statistical

significance was then determined using appropriate paired or unpaired Student's *t* test, ANOVA, or nonparametric tests. Statistical significance, denoted by asterisks (*) in figures, was considered at $P < 0.05$.

Supplementary Material

Refer to Web version on PubMed Central for supplementary material.

Acknowledgments

Funding: This work was supported by NIH grants R01 NS078792, R01 MH097887, and R01 AG055357 (to J.W.H.), R01 HL098200 and R01 HL121059 (to M.F.N.), R01 HL085372 (to W.A.C.), and F31 NS086226 (to O.R.B.); DFG HO 579/24-1 (to F.H.); AHA 11POST7020009 (to L.M.) and 16POST26560000 (to D.C.); P20 GM103492 (to M.A.N.); and Brain and Behavior Research Foundation NARSAD Young Investigator Grant 20748 (to L.M.).

REFERENCES AND NOTES

1. Hell JW, Westenbroek RE, Warner C, Ahlijanian MK, Prystay W, Gilbert MM, Snutch TP, Catterall WA. Identification and differential subcellular localization of the neuronal class C and class D L-type calcium channel alpha 1 subunits. J Cell Biol. 1993; 123:949–962. [PubMed: 8227151]
2. Dai S, Hall DD, Hell JW. Supramolecular assemblies and localized regulation of voltage-gated ion channels. Physiol Rev. 2009; 89:411–452. [PubMed: 19342611]
3. Sinnegger-Brauns MJ, Hetzenauer A, Huber IG, Renström E, Wietzorrek G, Berjukov S, Cavalli M, Walter D, Koschak A, Waldschütz R, Hering S, Bova S, Rorsman P, Pongs O, Singewald N, Striessnig J. Isoform-specific regulation of mood behavior and pancreatic β cell and cardiovascular function by L-type Ca^{2+} channels. J Clin Invest. 2004; 113:1430–1439. [PubMed: 15146240]
4. Navedo MF, Amberg GC. Local regulation of L-type Ca^{2+} channel sparklets in arterial smooth muscle. Microcirculation. 2013; 20:290–298. [PubMed: 23116449]
5. Splawski I, Timothy KW, Sharpe LM, Decher N, Kumar P, Bloise R, Napolitano C, Schwartz PJ, Joseph RM, Condouris K, Tager-Flusberg H, Priori SG, Sanguinetti MC, Keating MT. $Ca_V1.2$ calcium channel dysfunction causes a multisystem disorder including arrhythmia and autism. Cell. 2004; 119:19–31. [PubMed: 15454078]
6. Berkefeld H, Sailer CA, Bildl W, Rohde V, Thumfart JO, Eble S, Klugbauer N, Reisinger E, Bischofberger J, Oliver D, Knaus HG, Schulte U, Fakler B. BK_{Ca}-Cav channel complexes mediate rapid and localized Ca^{2+}-activated K^+ signaling. Science. 2006; 314:615–620. [PubMed: 17068255]
7. Marrion NV, Tavalin ST. Selective activation of Ca^{2+}-activated K^+ channels by co-localized Ca^{2+} channels in hippocampal neurons. Nature. 1998; 395:900–905. [PubMed: 9804423]
8. Dolmetsch RE, Pajvani U, Fife K, Spotts JM, Greenberg ME. Signaling to the nucleus by an L-type calcium channel-calmodulin complex through the MAP kinase pathway. Science. 2001; 294:333–339. [PubMed: 11598293]
9. Li H, Pink MD, Murphy JG, Stein A, Dell'Acqua ML, Hogan PG. Balanced interactions of calcineurin with AKAP79 regulate Ca^{2+}–calcineurin–NFAT signaling. Nat Struct Mol Biol. 2012; 19:337–345. [PubMed: 22343722]
10. Marshall MR, Clark JP III, Westenbroek R, Yu FH, Scheuer T, Catterall WA. Functional roles of a C-terminal signaling complex of Ca_V1 channels and A-kinase anchoring protein 15 in brain neurons. J Biol Chem. 2011; 286:12627–12639. [PubMed: 21224388]
11. Ma H, Groth RD, Cohen SM, Emery JF, Li B, Hoedt E, Zhang G, Neubert TA, Tsien RW. γCaMKII Shuttles Ca^{2+}/CaM to the nucleus to trigger CREB phosphorylation and gene expression. Cell. 2014; 159:281–294. [PubMed: 25303525]
12. Malenka RC, Bear MF. LTP and LTD: An embarrassment of riches. Neuron. 2004; 44:5–21. [PubMed: 15450156]
13. Collingridge GL, Isaac JTR, Wang YT. Receptor trafficking and synaptic plasticity. Nat Rev Neurosci. 2004; 5:952–962. [PubMed: 15550950]

14. Huganir RL, Nicoll RA. AMPARs and synaptic plasticity: The last 25 years. Neuron. 2013; 80:704–717. [PubMed: 24183021]
15. Grover LM, Teyler TJ. Two components of long-term potentiation induced by different patterns of afferent activation. Nature. 1990; 347:477–479. [PubMed: 1977084]
16. Moosmang S, Haider N, Klugbauer N, Adelsberger H, Langwieser N, Müller J, Stiess M, Marais E, Schulla V, Lacinova L, Goebbels S, Nave KA, Storm DR, Hofmann F, Kleppisch T. Role of hippocampal $Ca_v1.2$ Ca^{2+} channels in NMDA receptor-independent synaptic plasticity and spatial memory. J Neurosci. 2005; 25:9883–9892. [PubMed: 16251435]
17. Patriarchi T, Qian H, Di Biase V, Malik ZA, Chowdhury D, Price JL, Hammes EA, Buonarati OR, Westenbroek RE, Catterall WA, Hofmann F, Xiang YK, Murphy GG, Chen CY, Navedo MF, Hell JW. Phosphorylation of $Ca_v1.2$ on S1928 uncouples the L-type Ca^{2+} channel from the β_2 adrenergic receptor. EMBO J. 2016; 35:1330–1345. [PubMed: 27103070]
18. Bolshakov VY, Siegelbaum SA. Postsynaptic induction and presynaptic expression of hippocampal long-term depression. Science. 1994; 264:1148–1152. [PubMed: 7909958]
19. Berman DE, Dudai Y. Memory extinction, learning anew, and learning the new: Dissociations in the molecular machinery of learning in cortex. Science. 2001; 291:2417–2419. [PubMed: 11264539]
20. Cahill L, Prins B, Weber M, McGaugh JL. β-Adrenergic activation and memory for emotional events. Nature. 1994; 371:702–704. [PubMed: 7935815]
21. Carter ME, Yizhar O, Chikahisa S, Nguyen H, Adamantidis A, Nishino S, Deisseroth K, de Lecea L. Tuning arousal with optogenetic modulation of locus coeruleus neurons. Nat Neurosci. 2010; 13:1526–1533. [PubMed: 21037585]
22. Hu H, Real E, Takamiya K, Kang MG, Ledoux J, Huganir RL, Malinow R. Emotion enhances learning via norepinephrine regulation of AMPA-receptor trafficking. Cell. 2007; 131:160–173. [PubMed: 17923095]
23. Minzenberg MJ, Watrous AJ, Yoon JH, Ursu S, Carter CS. Modafinil shifts human locus coeruleus to low-tonic, high-phasic activity during functional MRI. Science. 2008; 322:1700–1702. [PubMed: 19074351]
24. Sanderson JL, Dell'Acqua ML. AKAP signaling complexes in regulation of excitatory synaptic plasticity. Neuroscientist. 2011; 17:321–336. [PubMed: 21498812]
25. Davare MA, Avdonin V, Hall DD, Peden EM, Burette A, Weinberg RJ, Horne MC, Hoshi T, Hell JW. A_{2+} β_2 adrenergic receptor signaling complex assembled with the Ca channel $Ca_v1.2$. Science. 2001; 293:98–101. [PubMed: 11441182]
26. Dittmer PJ, Dell'Acqua ML, Sather WA. Ca^{2+}/calcineurin-dependent inactivation of neuronal L-Type Ca^{2+} channels requires priming by AKAP-anchored protein kinase A. Cell Rep. 2014; 7:1410–1416. [PubMed: 24835998]
27. Gray R, Johnston D. Noradrenaline and β-adrenoceptor agonists increase activity of voltage-dependent calcium channels in hippocampal neurons. Nature. 1987; 327:620–622. [PubMed: 2439913]
28. Oliveria SF, Dell'Acqua ML, Sather WA. AKAP79/150 anchoring of calcineurin controls neuronal L-type Ca^{2+} channel activity and nuclear signaling. Neuron. 2007; 55:261–275. [PubMed: 17640527]
29. Balijepalli RC, Foell JD, Hall DD, Hell JW, Kamp TJ. Localization of cardiac L-type $Ca2^{+}$ channels to a caveolar macromolecular signaling complex is required for β_2-adrenergic regulation. Proc Natl Acad Sci USA. 2006; 103:7500–7505. [PubMed: 16648270]
30. Reuter H. Calcium channel modulation by neurotransmitters, enzymes and drugs. Nature. 1983; 301:569–574. [PubMed: 6131381]
31. Catterall WA. Structure and regulation of voltage-gated Ca^{2+} channels. Annu Rev Cell Dev Biol. 2000; 16:521–555. [PubMed: 11031246]
32. Sculptoreanu A, Rotman E, Takahashi M, Scheuer T, Catterall WA. Voltage-dependent potentiation of the activity of cardiac L-type calcium channel alpha 1 subunits due to phosphorylation by cAMP-dependent protein kinase. Proc Natl Acad Sci USA. 1993; 90:10135–10139. [PubMed: 7694283]

33. De Jongh KS, Murphy BJ, Colvin AA, Hell JW, Takahashi M, Catterall WA. Specific phosphorylation of a site in the full length form of the α1 subunit of the cardiac L-type calcium channel by adenosine 3‘,5‘-cyclic monophosphate-dependent protein kinase. Biochemistry. 1996; 35:10392–10402. [PubMed: 8756695]
34. Hell JW, Yokoyama CT, Wong ST, Warner C, Snutch TP, Catterall WA. Differential phosphorylation of two size forms of the neuronal class C L-type calcium channel α1 subunit. J Biol Chem. 1993; 268:19451–19457. [PubMed: 8396138]
35. Davare MA, Dong F, Rubin CS, Hell JW. The A-kinase anchor protein MAP2B and cAMP-dependent protein kinase are associated with class C L-type calcium channels in neurons. J Biol Chem. 1999; 274:30280–30287. [PubMed: 10514522]
36. Davare MA, Horne MC, Hell JW. Protein phosphatase 2A is associated with class C L-type calcium channels ($Ca_V1.2$) and antagonizes channel phosphorylation by cAMP-dependent protein kinase. J Biol Chem. 2000; 275:39710–39717. [PubMed: 10984483]
37. Hulme JT, Westenbroek RE, Scheuer T, Catterall WA. Phosphorylation of serine 1928 in the distal C-terminal domain of cardiac $Ca_V1.2$ channels during β1-adrenergic regulation. Proc Natl Acad Sci USA. 2006; 103:16574–16579. [PubMed: 17053072]
38. Hall DD, Davare MA, Shi M, Allen ML, Weisenhaus M, McKnight GS, Hell JW. Critical role of cAMP-dependent protein kinase anchoring to the L-type calcium channel $Ca_V1.2$ via A-kinase anchor protein 150 in neurons. Biochemistry. 2007; 46:1635–1646. [PubMed: 17279627]
39. Hell JW, Yokoyama CT, Breeze LJ, Chavkin C, Catterall WA. Phosphorylation of presynaptic and postsynaptic calcium channels by cAMP-dependent protein kinase in hippocampal neurons. EMBO J. 1995; 14:3036–3044. [PubMed: 7621818]
40. Davare MA, Hell JW. Increased phosphorylation of the neuronal L-type Ca^{2+} channel $Ca_V1.2$ during aging. Proc Natl Acad Sci USA. 2003; 100:16018–16023. [PubMed: 14665691]
41. Fuller MD, Emrick MA, Sadilek M, Scheuer T, Catterall WA. Molecular mechanism of calcium channel regulation in the fight-or-flight response. Sci Signal. 2010; 3:ra70. [PubMed: 20876873]
42. Ganesan AN, Maack C, Johns DC, Sidor A, O’Rourke B. β-Adrenergic stimulation of L-type Ca^{2+} channels in cardiac myocytes requires the distal carboxyl terminus of α_{1C} but not serine 1928. Circ Res. 2006; 98:e11–e18. [PubMed: 16397147]
43. Lemke T, Welling A, Christel CJ, Blaich A, Bernhard D, Lenhardt P, Hofmann F, Moosmang S. Unchanged β-adrenergic stimulation of cardiac L-type calcium channels in $Ca_V1.2$ phosphorylation site S1928A mutant mice. J Biol Chem. 2008; 283:34738–34744. [PubMed: 18829456]
44. Nichols CB, Rossow CF, Navedo MF, Westenbroek RE, Catterall WA, Santana LF, McKnight GS. Sympathetic stimulation of adult cardiomyocytes requires association of AKAP5 with a subpopulation of L-type calcium channels. Circ Res. 2010; 107:747–756. [PubMed: 20671242]
45. Murphy JG, Sanderson JL, Gorski JA, Scott JD, Catterall WA, Sather WA, Dell’Acqua ML. AKAP-anchored PKA maintains neuronal L-type calcium channel activity and NFAT transcriptional signaling. Cell Rep. 2014; 7:1577–1588. [PubMed: 24835999]
46. Fu Y, Westenbroek RE, Yu FH, Clark JP III, Marshall MR, Scheuer T, Catterall WA. Deletion of the distal C terminus of $Ca_V1.2$ channels leads to loss of β-adrenergic regulation and heart failure in vivo. J Biol Chem. 2011; 286:12617–12626. [PubMed: 21216955]
47. Hulme JT, Lin TW, Westenbroek RE, Scheuer T, Catterall WA. β-Adrenergic regulation requires direct anchoring of PKA to cardiac $Ca_V1.2$ channels via a leucine zipper interaction with A kinase-anchoring protein 15. Proc Natl Acad Sci USA. 2003; 100:13093–13098. [PubMed: 14569017]
48. Chen-Izu Y, Xiao RP, Izu LT, Cheng H, Kuschel M, Spurgeon H, Lakatta EG. G_i-dependent localization of β_2-adrenergic receptor signaling to L-type Ca^{2+} channels. Biophys J. 2000; 79:2547–2556. [PubMed: 11053129]
49. Xiao RP, Lakatta EG. β_1-Adrenoceptor stimulation and β_2-adrenoceptor stimulation differ in their effects on contraction, cytosolic Ca^{2+}, and Ca^{2+} current in single rat ventricular cells. Circ Res. 1993; 73:286–300. [PubMed: 8101141]

50. Hool LC, Harvey RD. Role of β_1- and β_2-adrenergic receptors in regulation of Cl^- and Ca^{2+} channels in guinea pig ventricular myocytes. Am J Physiol. 1997; 273:H1669–H1676. [PubMed: 9362229]
51. Nagykaldi Z, Kem D, Lazzara R, Szabo B. Canine ventricular myocyte β_2-adrenoceptors are not functionally coupled to L-type calcium current. J Cardiovasc Electrophysiol. 1999; 10:1240–1251. [PubMed: 10517658]
52. MacDougall DA, Agarwal SR, Stopford EA, Chu H, Collins JA, Longster AL, Colyer J, Harvey RD, Calaghan S. Caveolae compartmentalise β_2-adrenoceptor signals by curtailing cAMP production and maintaining phosphatase activity in the sarcoplasmic reticulum of the adult ventricular myocyte. J Mol Cell Cardiol. 2012; 52:388–400. [PubMed: 21740911]
53. Qian H, Matt L, Zhang M, Nguyen M, Patriarchi T, Koval ON, Anderson ME, He K, Lee HK, Hell JW. β_2-Adrenergic receptor supports prolonged theta tetanus-induced LTP. J Neurophysiol. 2012; 107:2703–2712. [PubMed: 22338020]
54. Joiner, M-lA, Lisé, M-F., Yuen, EY., Kam, AYF., Zhang, M., Hall, DD., Malik, ZA., Qian, H., Chen, Y., Ulrich, JD., Burette, AC., Weinberg, RJ., Law, PY., El-Husseini, A., Yan, Z., Hell, JW. Assembly of a β_2-adrenergic receptor—GluR1 signalling complex for localized cAMP signalling. EMBO J. 2010; 29:482–495. [PubMed: 19942860]
55. Wang D, Govindaiah G, Liu R, De Arcangelis V, Cox CL, Xiang YK. Binding of amyloid β peptide to β_2 adrenergic receptor induces PKA-dependent AMPA receptor hyperactivity. FASEB J. 2010; 24:3511–3521. [PubMed: 20395454]
56. Banke TG, Bowie D, Lee H, Huganir RL, Schousboe A, Traynelis SF. Control of GluR1 AMPA receptor function by cAMP-dependent protein kinase. J Neurosci. 2000; 20:89–102. [PubMed: 10627585]
57. Hayashi Y, Shi SH, Esteban JA, Piccini A, Poncer JC, Malinow R. Driving AMPA receptors into synapses by LTP and CaMKII: Requirement for GluR1 and PDZ domain interaction. Science. 2000; 287:2262–2267. [PubMed: 10731148]
58. Ehlers MD. Reinsertion or degradation of AMPA receptors determined by activity-dependent endocytic sorting. Neuron. 2000; 28:511–525. [PubMed: 11144360]
59. Lee HK, Barbarosie M, Kameyama K, Bear MF, Huganir RL. Regulation of distinct AMPA receptor phosphorylation sites during bidirectional synaptic plasticity. Nature. 2000; 405:955–959. [PubMed: 10879537]
60. Esteban JA, Shi SH, Wilson C, Nuriya M, Huganir RL, Malinow R. PKA phosphorylation of AMPA receptor subunits controls synaptic trafficking underlying plasticity. Nat Neurosci. 2003; 6:136–143. [PubMed: 12536214]
61. Lee HK, Takamiya K, He K, Song L, Huganir RL. Specific roles of AMPA receptor subunit GluR1 (GluA1) phosphorylation sites in regulating synaptic plasticity in the CA1 region of hippocampus. J Neurophysiol. 2010; 103:479–489. [PubMed: 19906877]
62. Sanderson JL, Gorski JA, Gibson ES, Lam P, Freund RK, Chick WS, Dell'Acqua ML. AKAP150-anchored calcineurin regulates synaptic plasticity by limiting synaptic incorporation of Ca^{2+}-permeable AMPA receptors. J Neurosci. 2012; 32:15036–15052. [PubMed: 23100425]
63. Sanderson JL, Gorski JA, Dell'Acqua ML. NMDA receptor-dependent LTD requires transient synaptic incorporation of Ca^{2+}-permeable AMPARs mediated by AKAP150-anchored PKA and calcineurin. Neuron. 2016; 89:1000–1015. [PubMed: 26938443]
64. Keith DJ, Sanderson JL, Gibson ES, Woolfrey KM, Robertson HR, Olszewski K, Kang R, El-Husseini A, Dell'Acqua ML. Palmitoylation of A-kinase anchoring protein 79/150 regulates dendritic endosomal targeting and synaptic plasticity mechanisms. J Neurosci. 2012; 32:7119–7136. [PubMed: 22623657]
65. Zhang M, Patriarchi T, Stein IS, Qian H, Matt L, Nguyen M, Xiang YK, Hell JW. Adenylyl cyclase anchoring by a kinase anchor protein AKAP5 (AKAP79/150) is important for postsynaptic β-adrenergic signaling. J Biol Chem. 2013; 288:17918–17931. [PubMed: 23649627]
66. Lu Y, Allen M, Halt AR, Weisenhaus M, Dallapiazza RF, Hall DD, Usachev YM, McKnight GS, Hell JW. Age-dependent requirement of AKAP150-anchored PKA and GluR2-lacking AMPA receptors in LTP. EMBO J. 2007; 26:4879–4890. [PubMed: 17972919]

67. Lu Y, Zhang M, Lim IA, Hall DD, Allen ML, Medvedeva Y, McKnight GS, Usachev YM, Hell JW. AKAP150-anchored PKA activity is important for LTD during its induction phase. J Physiol. 2008; 586:4155–4164. [PubMed: 18617570]
68. Skeberdis VA, Chevaleyre V, Lau CG, Goldberg JH, Pettit DL, Suadicani SO, Lin Y, Bennett MVL, Yuste R, Castillo PE, Zukin RS. Protein kinase A regulates calcium permeability of NMDA receptors. Nat Neurosci. 2006; 9:501–510. [PubMed: 16531999]
69. Murphy JA, Stein IS, Lau CG, Peixoto RT, Aman TK, Kaneko N, Aromolaran K, Saulnier JL, Popescu GK, Sabatini BL, Hell JW, Zukin RS. Phosphorylation of Ser1166 on GluN2B by PKA is critical to synaptic NMDA receptor function and Ca^{2+} signaling in spines. J Neurosci. 2014; 34:869–879. [PubMed: 24431445]
70. Thomas MJ, Moody TD, Makhinson M, O'Dell TJ. Activity-dependent beta-adrenergic modulation of low frequency stimulation induced LTP in the hippocampal CA1 region. Neuron. 1996; 17:475–482. [PubMed: 8816710]
71. Gelinas JN, Nguyen PV. β-Adrenergic receptor activation facilitates induction of a protein synthesis-dependent late phase of long-term potentiation. J Neurosci. 2005; 25:3294–3303. [PubMed: 15800184]
72. Mizuseki K, Sirota A, Pastalkova E, Buzsáki G. Theta oscillations provide temporal windows for local circuit computation in the entorhinal-hippocampal loop. Neuron. 2009; 64:267–280. [PubMed: 19874793]
73. Hoogland TM, Saggau P. Facilitation of L-type Ca^{2+} channels in dendritic spines by activation of β_2 adrenergic receptors. J Neurosci. 2004; 24:8416–8427. [PubMed: 15456814]
74. Hell JW. β-Adrenergic regulation of the L-type Ca^{2+} channel $Ca_V1.2$ by PKA rekindles excitement. Sci Signal. 2010; 3:pe33. [PubMed: 20876870]
75. Fu Y, Westenbroek RE, Scheuer T, Catterall WA. Phosphorylation sites required for regulation of cardiac calcium channels in the fight-or-flight response. Proc Natl Acad Sci USA. 2013; 110:19621–19626. [PubMed: 24218620]
76. Fu Y, Westenbroek RE, Scheuer T, Catterall WA. Basal and β-adrenergic regulation of the cardiac calcium channel $Ca_V1.2$ requires phosphorylation of serine 1700. Proc Natl Acad Sci USA. 2014; 111:16598–16603. [PubMed: 25368181]
77. Bean BP, Nowycky MC, Tsien RW. β-Adrenergic modulation of calcium channels in frog ventricular heart cells. Nature. 1984; 307:371–375. [PubMed: 6320002]
78. Catterall WA. Regulation of cardiac calcium channels in the fight-or-flight response. Curr Mol Pharmacol. 2015; 8:12–21. [PubMed: 25966697]
79. Nystoriak MA, Nieves-Cintrón M, Patriarchi T, Buonarati OR, Prada MP, Morroti S, Grandi E, Fernandes JDS, Forbush K, Hofmann F, Sasse KC, Scott JD, Ward SM, Hell JW, Navedo MF. Ser^{1928} phosphorylation by PKA stimulates the L-type Ca^{2+} channel $Ca_V1.2$ and vasoconstriction during acute hyperglycemia and diabetes. Sci Signal. 2017; 10:eaaf9647. [PubMed: 28119464]
80. Makarewich CA, Correll RN, Gao H, Zhang H, Yang B, Berretta RM, Rizzo V, Molkentin JD, Houser SR. A caveolae-targeted L-type Ca^{2+} channel antagonist inhibits hypertrophic signaling without reducing cardiac contractility. Circ Res. 2012; 110:669–674. [PubMed: 22302787]
81. Nobles KN, Xiao K, Ahn S, Shukla AK, Lam CM, Rajagopal S, Strachan RT, Huang TY, Bressler EA, Hara MR, Shenoy SK, Gygi SP, Lefkowitz RJ. Distinct phosphorylation sites on the β_2-adrenergic receptor establish a barcode that encodes differential functions of β-arrestin. Sci Signal. 2011; 4:ra51. [PubMed: 21868357]
82. Reiter E, Ahn S, Shukla AK, Lefkowitz RJ. Molecular mechanism of β-arrestin-biased agonism at seven-transmembrane receptors. Annu Rev Pharmacol Toxicol. 2012; 52:179–197. [PubMed: 21942629]
83. Foell JD, Balijepalli RC, Delisle BP, Yunker AM, Robia SL, Walker JW, McEnery MW, January CT, Kamp TJ. Molecular heterogeneity of calcium channel β-subunits in canine and human heart: Evidence for differential subcellular localization. Physiol Genomics. 2004; 17:183–200. [PubMed: 14762176]
84. Zamponi GW, Striessnig J, Koschak A, Dolphin AC. The physiology, pathology, and pharmacology of voltage-gated calcium channels and their future therapeutic potential. Pharmacol Rev. 2015; 67:821–870. [PubMed: 26362469]

85. Colecraft HM, Alseikhan B, Takahashi SX, Chaudhuri D, Mittman S, Yegnasubramanian V, Alvania RS, Johns DC, Marban E, Yue DT. Novel functional properties of Ca^{2+} channel β subunits revealed by their expression in adult rat heart cells. J Physiol. 2002; 541:435–452. [PubMed: 12042350]
86. Gerhardstein BL, Puri TS, Chien AJ, Hosey MM. Identification of the sites phosphorylated by cyclic AMP-dependent protein kinase on the β_2 subunit of L-type voltage-dependent calcium channels. Biochemistry. 1999; 38:10361–10370. [PubMed: 10441130]
87. Scott VES, De Waard M, Liu H, Gurnett CA, Venzke DP, Lennon VA, Campbell KP. β subunit heterogeneity in N-type Ca^{2+} channels. J Biol Chem. 1996; 271:3207–3212. [PubMed: 8621722]
88. Pichler M, Cassidy TN, Reimer D, Haase H, Kraus R, Ostler D, Striessnig J. β subunit heterogeneity in neuronal L-type Ca^{2+} channels. J Biol Chem. 1997; 272:13877–13882. [PubMed: 9153247]
89. Burgess DL, Biddlecome GH, McDonough SI, Diaz ME, Zilinski CA, Bean BP, Campbell KP, Noebels JL. β subunit reshuffling modifies N- and P/Q-type Ca^{2+} channel subunit compositions in lethargic mouse brain. Mol Cell Neurosci. 1999; 13:293–311. [PubMed: 10328888]
90. Mikami A, Imoto K, Tanabe T, Niidome T, Mori Y, Takeshima H, Narumiya S, Numa S. Primary structure and functional expression of the cardiac dihydropyridine-sensitive calcium channel. Nature. 1989; 340:230–233. [PubMed: 2474130]
91. Snutch TP, Tomlinson WJ, Leonard JP, Gilbert MM. Distinct calcium channels are generated by alternative splicing and are differentially expressed in the mammalian CNS. Neuron. 1991; 7:45–57. [PubMed: 1648941]
92. Hell JW, Westenbroek RE, Breeze LJ, Wang KKW, Chavkin C, Catterall WA. *N*-methyl-D-aspartate receptor-induced proteolytic conversion of postsynaptic class C L-type calcium channels in hippocampal neurons. Proc Natl Acad Sci USA. 1996; 93:3362–3367. [PubMed: 8622942]
93. Fuller MD, Fu Y, Scheuer T, Catterall WA. Differential regulation of $Ca_V1.2$ channels by cAMP-dependent protein kinase bound to A-kinase anchoring proteins 15 and 79/150. J Gen Physiol. 2014; 143:315–324. [PubMed: 24567507]
94. Leonard AS, Davare MA, Horne MC, Garner CC, Hell JW. SAP97 is associated with the α-amino-3-hydroxy-5-methylisoxazole-4-propionic acid receptor GluR1 subunit. J Biol Chem. 1998; 273:19518–19524. [PubMed: 9677374]
95. Efendiev R, Samelson BK, Nguyen BT, Phatarpekar PV, Baameur F, Scott JD, Dessauer CW. AKAP79 interacts with multiple adenylyl cyclase (AC) isoforms and scaffolds AC5 and -6 to α-amino-3-hydroxyl-5-methyl-4-isoxazole-propionate (AMPA) receptors. J Biol Chem. 2010; 285:14450–14458. [PubMed: 20231277]
96. Colledge M, Dean RA, Scott GK, Langeberg LK, Huganir RL, Scott JD. Targeting of PKA to glutamate receptors through a MAGUK-AKAP complex. Neuron. 2000; 27:107–119. [PubMed: 10939335]
97. Tavalin SJ, Colledge M, Hell JW, Langeberg LK, Huganir RL, Scott JD. Regulation of GluR1 by the A-kinase anchoring protein 79 (AKAP79) signaling complex shares properties with long-term depression. J Neurosci. 2002; 22:3044–3051. [PubMed: 11943807]
98. Robertson HR, Gibson ES, Benke TA, Dell'Acqua ML. Regulation of postsynaptic structure and function by an A-kinase anchoring protein-membrane-associated guanylate kinase scaffolding complex. J Neurosci. 2009; 29:7929–7943. [PubMed: 19535604]
99. Hall DD, Feekes JA, Arachchige Don AS, Shi M, Hamid J, Chen L, Strack S, Zamponi GW, Horne MC, Hell JW. Binding of protein phosphatase 2A to the L-type calcium channel $Ca_V1.2$ next to Ser1928, its main PKA site, is critical for Ser1928 dephosphorylation. Biochemistry. 2006; 45:3448–3459. [PubMed: 16519540]
100. Chen Y, Stevens B, Chang J, Milbrandt J, Barres BA, Hell JW. NS21: Re-defined and modified supplement B27 for neuronal cultures. J Neurosci Methods. 2008; 171:239–247. [PubMed: 18471889]
101. Hall DD, Dai S, Tseng P-Y, Malik ZA, Nguyen M, Matt L, Schnizler K, Shephard A, Mohapatra D, Tsuruta F, Dolmetsch RE, Christel CJ, Lee A, Burette A, Weinberg RJ, Hell JW. Competition between α-actinin and Ca^{2+}-calmodulin controls surface retention of the L-type Ca^{2+} channel $Ca_V1.2$. Neuron. 2013; 78:483–497. [PubMed: 23664615]

102. Halt AR, Dallapiazza R, Yu H, Stein IS, Qian H, Junti S, Wojcik S, Brose N, Sliva A, Hell JW. CaMKII binding to GluN2B is critical during memory consolidation. EMBO J. 2012; 31:1203–1216. [PubMed: 22234183]

103. Alliance for Cellular Signaling (AfCS) Procedure Protocol PP00000125;. http://afcs.lbl.gov/reports/v1/CM0005/CM0005.pdf

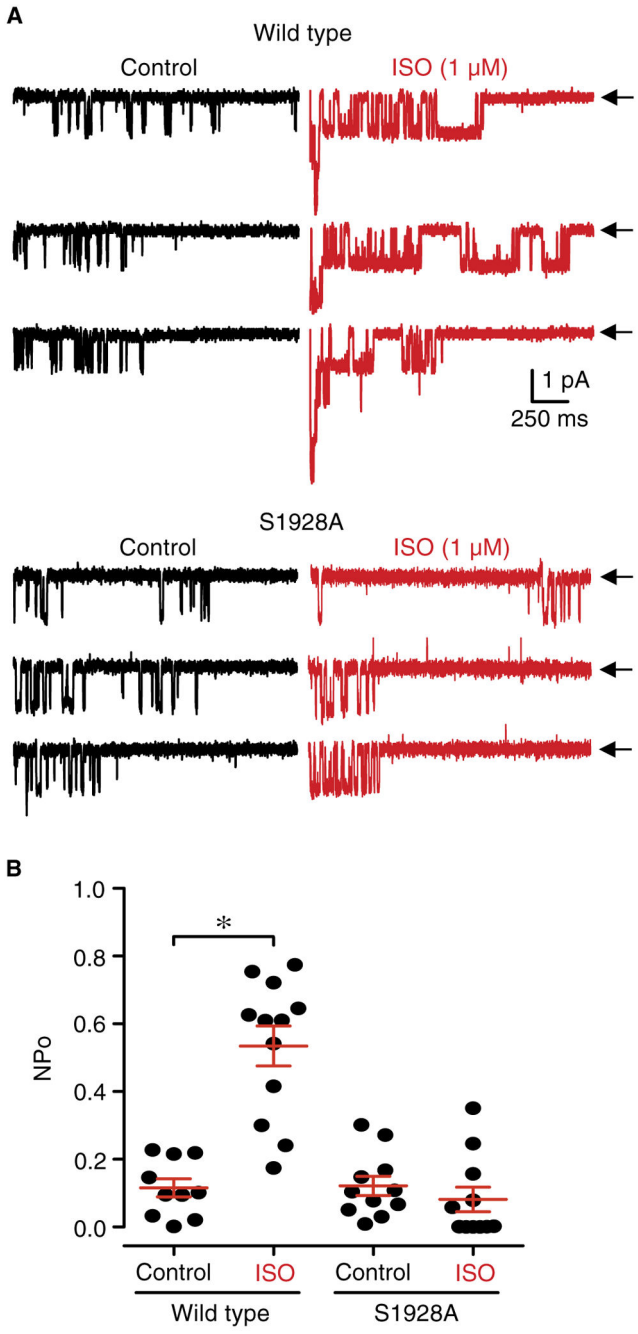

Fig. 1. βAR augmentation of L-type currents in neurons requires Ser^{1928}

(**A**) Representative single-channel recordings from hippocampal neurons from wild-type and litter-matched S1928A KI mice at 7 to 14 days in vitro upon depolarization from −80 to 0 mV without (left, black traces) and with 1 μM ISO (right, red traces) in the patch pipette. Arrows (←) indicate the zero-current level (that is, the closed channel). (**B**) Summary plot of NPo recorded from neurons from wild-type and S1928A KI mice with vehicle (H_2O) or 1 μM ISO added to the patch pipette solution. For statistical analysis, NPo was determined for each recording and pooled under each condition for comparison (*$P < 0.05$, unpaired *t* test

for experiments in wild-type cells and Mann-Whitney test for experiments in S1928A cells). Mean NPo values are 0.12 ± 0.03 for wild-type control (n = 10), 0.53 ± 0.06 for wild-type ISO (n = 12), 0.12 ± 0.03 for S1928A control (n = 11), and 0.08 ± 0.04 for S1928A ISO (n = 11) (n, number of cell-attached patch recordings pooled across three to five independent culture experiments).

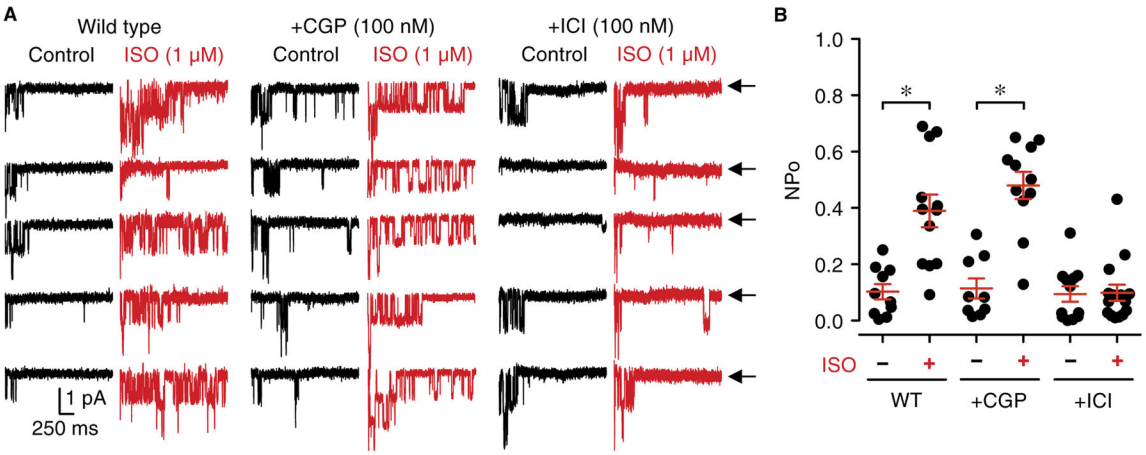

Fig. 2. β_2AR but not β_1AR signaling augments L-type currents in neurons

(**A**) Representative single-channel recordings from wild-type (WT) rat hippocampal neurons. The patch pipette solution contained vehicle (H_2O; control; −) or 1 μM ISO (+; red traces) plus 100 nM CGP20712 (+CGP) or 100 nM ICI118551 (+ICI). Arrows throughout the figure (←) indicate the zero-current level (closed channel). (**B**) Summary plot for data in (A). For statistical analysis, the NPo value was determined for each recording and pooled under each condition for comparison (*$P < 0.05$; unpaired *t* test was used to compare statistical significance in wild-type cells under control conditions with those treated with CGP. Mann-Whitney test was used in cells treated with ICI). Average NPo values are 0.10 ± 0.03 for wild type – ISO ($n = 10$), 0.39 ± 0.06 for wild type + ISO ($n = 12$), 0.11 ± 0.04 for CGP – ISO ($n = 9$), 0.48 ± 0.05 for CGP + ISO ($n = 11$), 0.09 ± 0.03 for ICI – ISO ($n = 12$), and 0.10 ± 0.03 for ICI + ISO ($n = 15$) (*n*, number of cell-attached patch recordings from three independent culture experiments).

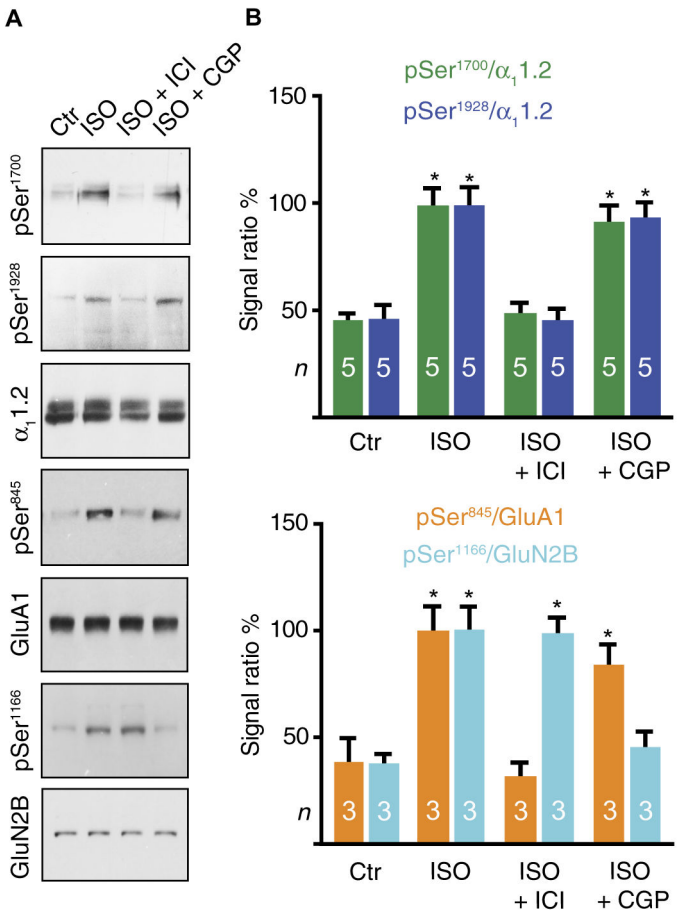

Fig. 3. β_2AR controls phosphorylation of $Ca_V1.2$ and GluA1, and β_1AR controls phosphorylation of GluN2B

(**A**) Forebrain slices from wild-type mice of either sex were treated with ASCF containing vehicle (H_2O; Ctr) or 1 μM ISO plus 100 nM ICI118551 (+ICI) or 100 nM CGP20712 (+CGP), as indicated, for 5 min before solubilization, ultracentrifugation, simultaneous immunoprecipitation (IP) of $\alpha_1$1.2 plus GluA1, and subsequent immunoprecipitation of GluN2B from supernatants resulting from the $\alpha_1$1.2/GluA1 immunoprecipitation. Samples were analyzed by sequential immunoblotting for phosphorylated Ser^{1928} ($pSer^{1928}$), $pSer^{1700}$, and $\alpha_1$1.2 (top panels) and for $pSer^{845}$ and GluA1 (middle panels) from the same blots and sequential immunoblot-ting for $pSer^{1166}$ and GluN2B of a second blot using corresponding regions of the blots. (**B**) For quantification of $\alpha_1$1.2 phosphorylation, $pSer^{1928}$ and $pSer^{1700}$ signals were nor-malized to total $\alpha_1$1.2 [$*P < 0.05$ versus control, analysis of variance (ANOVA) with Bonferroni correction for multiple testing between all experimental conditions; *n*, number of samples analyzed across three independent experiments]. For quantification of GluA1 phosphorylation, $pSer^{845}$ signals were normalized to GluA1 ($*P < 0.05$, ANOVA with Bonferroni's test; *n*, number of samples analyzed across three independent experiments). For quantification of GluN2B phosphorylation, $pSer^{1166}$ signals were normalized to GluN2B ($*P < 0.05$, ANOVA with Bonferroni correction for multiple testing; *n*, number of samples analyzed across three independent experiments).

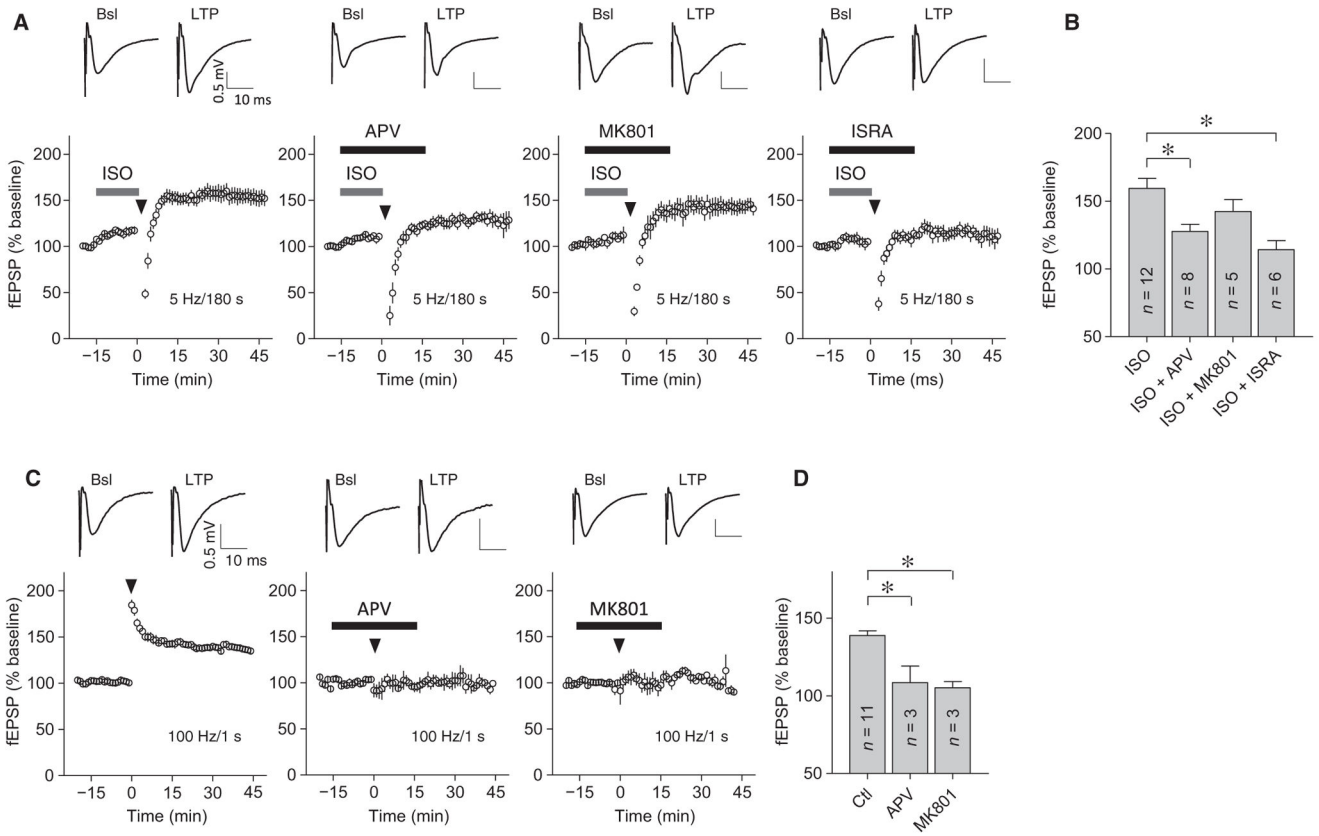

Fig. 4. L-type Ca^{2+} channels mediate PTT-LTP

Graphs show representative fEPSP initial slopes recorded from hippocampal CA1 and amalgamated data before [basal (Bsl)] and after either a 3-min, 5-Hz tetanus (**A** and **B**) or two 1-s, 100-Hz tetani (**C** and **D**). Arrowheads mark onset of tetani, gray bars indicate perfusion with 1 μM ISO, and black bars indicate perfusion with 50 μM DL-APV, 100 μM MK801, or 10 μM isradipine (ISRA), as indicated. Insets on top show sample traces immediately before (left) and ~30 min after (right) tetani. Degree of potentiation was determined 30 min after tetanus and compared to baseline before tetanus. PTT-LTP was 159.4 ± 7.4% of baseline for control conditions, 127.6 ± 5.3% for APV, 142.4 ± 8.7% for MK801, and 107.0 ± 4.1% for isradipine. LTP induced by two 100-Hz tetani was 138.9 ± 3.0% for control conditions, 108.6 ± 10.5% for APV, and 105.2 ± 4.0% for MK801 (*P < 0.05; Kruskal-Wallis with Dunn's test; n, number of slices from three to six mice of either sex used for n number of recordings).

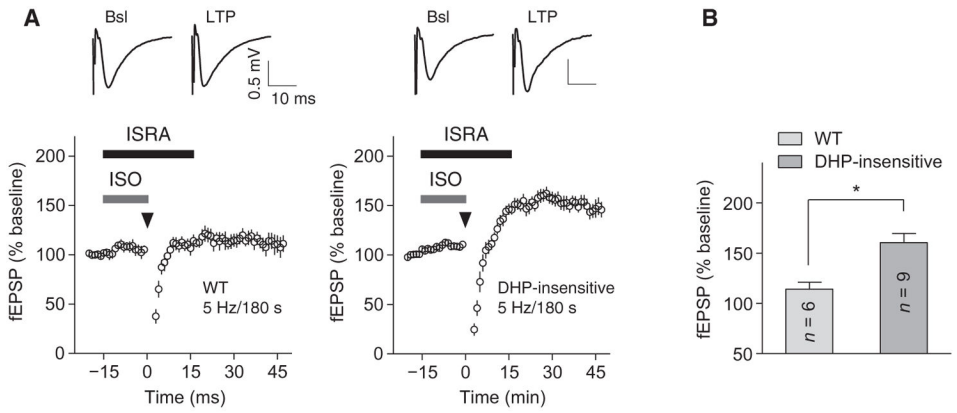

Fig. 5. PTT-LTP requires $Ca_v1.2$

Graphs show fEPSP initial slopes recorded from hippocampal slices from litter-matched wild-type mice and isradipine-insensitive (DHP) T1066Y KI mice (**A**) and amalgamated data (**B**). Arrowheads mark onset of the 3-min, 5-Hz tetanus, gray bars indicate perfusion with 1 μM ISO, and black bars indicate perfusion with 10 μM isradipine. Insets on top show sample traces immediately before (left) and ~30 min after (right) tetani. Degree of potentiation was determined 30 min after tetanus and compared to baseline before tetanus. Average fEPSP was 114.2 ± 6.8% of baseline in slices from wild-type mice and 160.4 ± 9.2% of baseline in slices from DHP-insensitive, T1066Y KI mice (*$P < 0.05$; Mann-Whitney test; *n*, number of slices for the same number of recordings; wild-type mice: three animals; isradipine-insensitive mice: six animals of either sex).

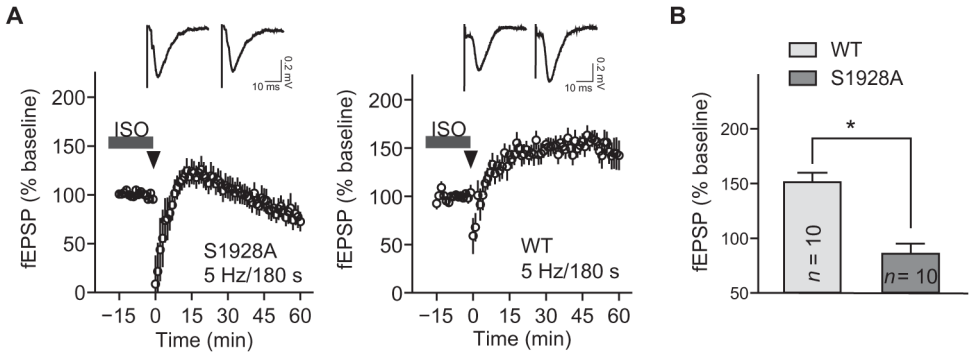

Fig. 6. PTT-LTP requires phosphorylation of $Ca_V1.2$ on Ser^{1928}

Graphs show fEPSP initial slopes recorded from hippocampal slices from litter-matched S1928A KI mice and wild-type mice (**A**) and amalgamated data (**B**). Arrowheads mark onset of the 5 Hz, 3 min tetanus, and gray bars indicate perfusion with 1 μM ISO. Insets on top show sample traces immediately before (left) and ~30 min after (right) tetani. Degree of potentiation was determined 30 min after tetanus and compared to baseline before tetanus. Average fEPSP was 151.3 ± 8.6% of baseline in slices from wild-type mice (**P* < 0.05 baseline versus tetanized; Mann-Whitney test) and 85.8 ± 9.3% of baseline in slices from S1928A KI mice (**P* < 0.05; Mann-Whitney test; *n*, number of slices for the same number of recordings; wild-type mice: six animals; S1928A KI mice: three animals of either sex)..

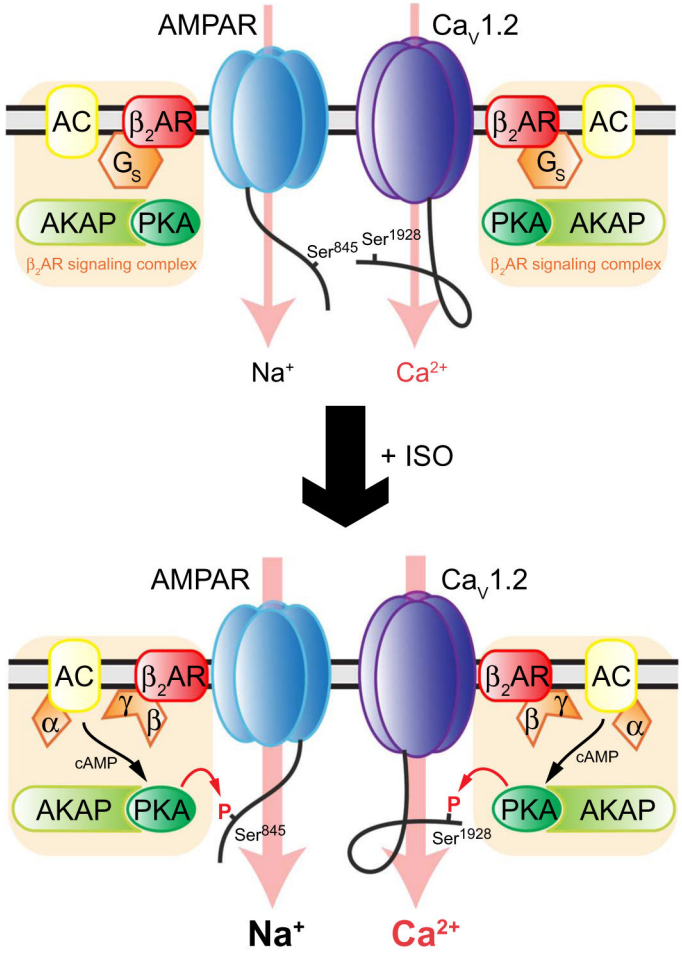

Fig. 7. Model for enhancement of Ca^{2+} influx through $Ca_V1.2$ during PTT-LTP

Under basal conditions, phosphorylation of Ser^{845} in the AMPAR GluA1 subunit and of Ser^{1928} in the $Ca_V1.2$ $\alpha_1$1.2 subunit and Ser^{1928} is low. Stimulation of AMPAR- and $Ca_V1.2$-associated β_2ARs activates G_s-mediated AC signaling and thereby cAMP production and PKA. The resulting Ser^{845} phosphorylation increases Po of the AMPAR, which results in Na^+ influx and depolarization during synaptic transmission induced by the theta stimulation. Ser^{1928} phosphorylation increases Po of $Ca_V1.2$ and thereby Ca^{2+} influx through this channel. This increase in Ca^{2+} influx through $Ca_V1.2$ triggers the potentiation of synaptic strength in PTT-LTP via yet-to-be-defined signaling pathways.